# RI 9068

Bureau of Mines Report of Investigations/1987

# Damping Properties of Selected Steels and Cast Irons

By A. Visnapuu, R. W. Nash, and P. C. Turner

UNITED STATES DEPARTMENT OF THE INTERIOR

Report of Investigations 9068

# Damping Properties of Selected Steels and Cast Irons

By A. Visnapuu, R. W. Nash, and P. C. Turner

**UNITED STATES DEPARTMENT OF THE INTERIOR**
Donald Paul Hodel, Secretary

**BUREAU OF MINES**
Robert C. Horton, Director

Library of Congress Cataloging in Publication Data:

**Visnapuu, A. (Aarne)**
Damping properties of selected steels and cast irons.

(Report of investigations ; 9068)

Bibliography: p. 14-15.

Supt. of Docs. no.: I 28.23: 9068.

1. Mining machinery - Vibration. 2. Steel - Testing. 3. Cast-iron - Testing. 4. Damping (Mechanics). I. Nash, R. W. (Robert W.). II. Turner, P. C. III. Title. IV. Series: Report of investigations (United States. Bureau of Mines) ; 9068.

TN23.U43 [TN345] 622 s [620.3] 86-600351

CONTENTS



ILLUSTRATIONS



TABLES

## UNIT OF MEASURE ABBREVIATIONS USED IN THIS REPORT

| | | | |
|---|---|---|---|
| °C | degree Celsius | Oe | oersted |
| °C/h | degree Celsius per hour | pct | percent |
| h | hour | lb | pound |
| Hz | hertz | psi | pound (force) per square inch |
| in | inch | vol pct | volume percent |
| lb/min | pound per minute | wt pct | weight percent |
| min | minute | | |

# DAMPING PROPERTIES OF SELECTED STEELS AND CAST IRONS

By A. Visnapuu,[1] R. W. Nash,[2] and P. C. Turner[3]

ABSTRACT

Excessive noise and high vibration are inherently associated with equipment used in the mining, extraction, and processing of mineral resources. High vibration degrades structural components, often leading to catastrophic failure and loss of productivity, and excessive noise can result in permanent hearing loss.

In order to foster efficient utilization of the Nation's mineral resources and minimize occupational hazards associated with mineral processing, the Bureau of Mines investigated the relationship between the microstructures of carbon and alloy steels and cast irons and their damping capacities (ability to absorb vibration). Researchers measured damping capacity and other properties and investigated the effects of carburizing, spheroidizing, and annealing.

The investigators found that in carbon and alloy steels, rounded colonies of fine-grained pearlite in a ferrite matrix correlate well with low damping capacity. Steel microstructures that exhibit sharp-faceted pearlite in ferrite matrix and partially or fully spheroidized cementite in ferrite show considerably higher damping. In cast irons, the lowest damping capacity is associated with nodular graphite microstructure, and the specific damping capacity (SDC) increases as the graphite microstructure progresses from nodular to compacted to flake. Predominant ferrite in cast irons is also associated with good damping. SDC data are presented for selected carbon and alloy steels and cast irons.

[1]Research physicist.
[2]Physical science technician.
[3]Metallurgist.
Rolla Research Center, Bureau of Mines, Rolla, MO.

## INTRODUCTION

In recent years, the vibration damping inherent in engineering materials has gained importance as a design consideration, in addition to the more commonly considered mechanical properties such as tensile and yield strength, ductility, hardness, and toughness. The need for improved damping properties, without undue sacrifice of other properties that determine durability, is the result of increased demand for lower product, workplace, and environmental noise, and the realization that reduced vibration can prolong the service life of machinery and equipment. One fundamental way to improve damping properties is to use relatively high-damping materials. Of the available structural alloy systems, only ferrous alloys appear to be cheap enough in intrinsic material and processing cost to be economically feasible.

## PREVIOUS INVESTIGATIONS

Previous investigations have developed a variety of damping materials and methods, and some have been developed to the point of commercial availability. Manganese-copper binary alloys ranging from 50 to 80 wt pct Mn, both cast (1)[4] and powder-metallurgy consolidated (2), exhibit SDC's in the range 20 to 25 pct at a stress of 5,000 psi. In addition to high damping capacity, these alloys have useful mechanical properties comparable to those of mild steel. High damping is obtained by solution heat treatment followed by aging to precipitate an intermetallic phase.

Other Mn-Cu-based damping alloys with minor metal additions have been developed. Sonoston[5] alloy has the composition Cu-54 Mn-4.25 Al-3 Fe-1.5 Ni (3). The damping alloys Incramute I and II, developed by the International Copper Research Association, consist of Cu-40 Mn-2 Al and Cu-40 Mn-2 Al-2 Sn, respectively (4-6). They are commercially available.

While the Mn-Cu alloys possess excellent vibration damping and good mechanical properties, they have some disadvantages: (1) The cost of component metals and fabrication is high, and (2) damping capacity decreases with temperature. Other low-strength materials are adequate for many applications. The Sonoston and Incramute I alloys lose their damping above 75° C. Damping in Incramute II disappears above about 125° C. The higher damping transition temperature for Incramute II is due to the tin addition, which apparently affects precipitate stability (4).

A ferromagnetic iron-base alloy containing chromium and aluminum, developed in Japan, is reported to have high damping up to 350° C (7). A drawback with this alloy is that damping capacity is dependent on an external magnetic field. Maximum damping requires an applied magnetic field of about 20 Oe. Another alloy, NIVCO-10, developed by Westinghouse Electric Corp., has good damping and excellent mechanical properties; however, its composition, Co-22.5 Ni-1.8 Ti, is high in the critical metals cobalt and nickel, which must be imported, meaning that its use must be restricted to special applications.

Alternate approaches for damping commonly use shock absorbers, shock mounts, constrained-layer damping, and bonded-on materials to isolate, increase mass, or increase stiffness. In many instances, these measures provide the most practical and economic damping method. Sometimes they are only partly effective but are used because engineering materials with the requisite damping and physical properties are not available or are cost-prohibitive. Some aluminum alloys and brass have SDC's on the order of 0.01 to 1 pct at stress levels below 3,500 psi.

Of the iron-based materials, gray cast irons exhibit excellent damping owing to energy dissipation resulting from high

---

[4] Underlined numbers in parentheses refer to items in the list of references at the end of this report.

[5] Reference to specific products does not imply endorsement by the Bureau of Mines.

stress concentrations around the embrittling graphite flakes (8); however, useful toughness is practically nil. This has limited the use of gray cast irons to applications where toughness is not a major factor. Ductile irons have nodular graphite dispersed in continuous matrices similar to those of steel, which imparts toughness and ductility and permits plastic deformation, but markedly reduces damping capacity relative to that of gray cast irons. Ductile irons are actually a family of materials; they differ as a result of factors such as composition, section size, cooling rate, and heat treatment, and can be processed into a wide range of properties (9-10). Compared with steels, ductile irons have generally inferior ductility, weldability, and impact and fatigue resistance, but superior castability, machinability, wear and corrosion resistance, and damping capacity. Compacted graphite cast irons have structures that are intermediate in terms of form, to the flakes of gray cast iron and the nodules of ductile iron. Graphite in compacted graphite cast iron has rounded tips, relative to the flakes in gray cast iron, but is continuous in the sense that flakes are continuous in the matrix (actually they are relatively long-range colonies on a microscopic scale). This graphite morphology, which may be associated with some graphite tending toward flakes or nodules, imparts certain desirable properties relative to gray cast iron, such as increased ductility and tensile and yield strength.

Steels tend to exhibit low SDC's in comparison with those of the cast irons, which is attributable to the absence of free graphite. Damping in steels increases somewhat with the carbon content, and spheroidization tends to further enhance damping capacity.

## PURPOSE OF THIS INVESTIGATION

This investigation was conducted as part of the Bureau's research effort to conserve resources and increase productivity through improved performance and develop safer materials. Baseline SDC's were determined for representative industrial and structural carbon steels and cast irons and were correlated to the respective carbide and graphite microstructures. Selected materials were subjected to carburizing, spheroidizing, and annealing heat treatments to delineate their influence on damping and other properties. The data reported is intended to supplement the meager damping capacity information available on these materials and to serve as a benchmark against which ongoing developmental work can be compared. The ultimate goal is to use this information to produce new iron-base high-damping materials or to alter the structure of existing materials to improve damping.

## EXPERIMENTAL PROCEDURE

The carbon and alloy steels investigated in this study were of the following AISI grades: 1020, 1035, 1045, 1095, 1117, 1144, 4140, and 4340. The steels were selected as being representative of commercially available steels. Specimens for measuring damping capacity and other physical properties were prepared from commercial hot-rolled rod stock that varied in diameter from 3/4 to 2-1/4 in. In addition to SDC evaluation in the as-received condition, measurements were made after selective heat treatment to alter the carbide morphology. Damping capacity specimens of the 1045, 1095, 1144, 4140, and 4340 steels were carburized for 3 h at 925° C using sodium carbonate, barium carbonate, and charcoal. The 1045, 1144, 4140, and 4340 steels were then given a spheroidizing heat treatment by holding at 750° C for 6 h, cooling at 30° C/h to 650° C, and holding at 650° C for 36 h. The 1095 steel was spheroidized by holding at 715° C for 6 h, followed by a 36-h hold at 680° C.

Cast irons were prepared in 60- and 120-lb heats by induction melting in magnesium oxide crucibles. The temperature was monitored with Pt, Pt-10 Rh thermocouples in protection tubes, and carbon equivalent was determined from the temperature of eutectic solidification. Heats were constituted to have nominally 2.4 to 3.0 pct Si, carbon equivalent from 4.2 to 4.8 pct, and 0.3 pct Mn. Magnesium or mischmetal (57 pct Ce) was added as a nodulizing agent, and titanium or zirconium was added separately as a denodulizing agent. Some of the 60-lb heats were made using a single additive containing both magnesium and titanium. All the cast iron heats were cast in standard keel-block molds (core sand) with 1-in legs. Ductile iron castings were ferritize-annealed by heating in helium for 3 h at 900° C, followed by cooling to and holding at 695° C for 6 h.

Tensile specimens with a standard 0.5-in diam (11) were prepared from keel-block legs and tested on a tensile test machine at a 4,800-lb/min load rate to yield. Tensile strength, 0.2-pct offset yield strength, and elongation (percent) were calculated.

Chemical analyses and microscopy were conventional. Carbon content was determined from pin castings and analyses of other elements from drillings. Microscopy specimens were polished with diamond abrasive and etched in nital (2 vol pct $HNO_3$ and 98 vol pct $C_2H_5OH$).

SDC was measured with a torsion pendulum designed and assembled by the Bureau (12-13). SDC is defined as

$$SDC = [(A_o{}^2 - A_n{}^2)/nA_o{}^2] \times 100,$$

where $A_o$ is the initial amplitude of torsional vibration at resonance and $A_n$ is the amplitude n cycles after $A_o$. Typical resonance frequencies for these specimens varied from 7 to 15 Hz due to differences in modulus of elasticity. The damping capacity is independent of frequency and mode of vibration (1). Although the results are reported as SDC, other descriptors of damping, such as loss factor, fraction of critical damping, logarithmic decrement, and half-power bandwidth, can be readily obtained from the data. The SDC measurements were made on shouldered specimens 4.5 in long with a 2.5-in gauge length and a 0.188-in reduced diameter. The curves of SDC versus torsional stress (presented in the next section) are digitally filtered curves derived from the 19 or more SDC values obtained for each specimen. The curves were generated by a sliding, 5-point curve-fitting computer routine.

## RESULTS AND DISCUSSION

### STEELS

The results of SDC measurements on the hot-rolled carbon and alloy steel rod stock are summarized in table 1. SDC's for each steel are tabulated at five stress levels ranging from 2,500 to 20,000 psi, with the steels listed in order of increasing damping in the 2,500- to 10,000-psi range. A brief description of the carbide morphology of each steel is included in table 1, and the corresponding microstructures are shown in figure 1. SDC-versus-stress curves representative of trends are presented in figure 2.

Comparison of the damping data (table 1) with the corresponding steel microstructures (fig. 1) indicates that the presence of rounded colonies of fine-grained lamellar pearlite or unresolved pearlite in a ferrite matrix correlates with low SDC, whereas steel microstructures that exhibit sharp-faceted pearlite colonies and relatively high proportions of coarse-grained pearlite in a ferrite matrix show considerably higher damping. This agrees with the theory that increased stress concentrations associated with sharp points at phase boundaries increase damping, as does a higher proportion of ferrite in the matrix. The AISI 1045, 1144, 1095, and 1117 steels, as a group, exhibited considerably lower damping than the remaining four steels listed in table 1. Their microstructures can be characterized as rounded colonies of fine lamellar pearlite in a ferrite matrix (1045 and 1144), mostly unresolved pearlite with some coarse lamellar spacing (1095), and rounded colonies of unresolved pearlite in an increased ferrite

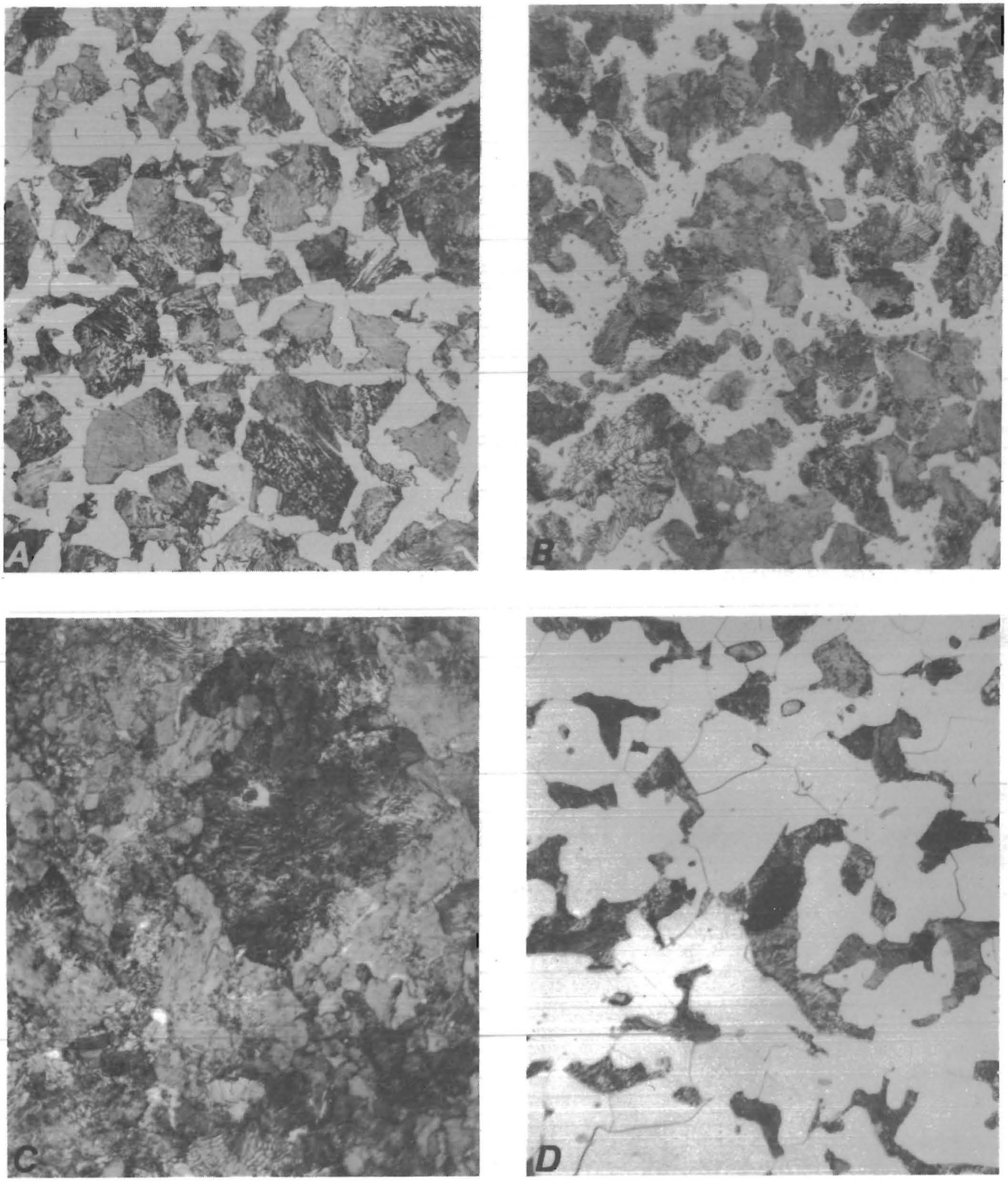


FIGURE 1.—Microstructures of carbon and alloy steels (X 500). AISI designations: *A*, 1045; *B*, 1144; *C*, 1095; *D*, 1117.

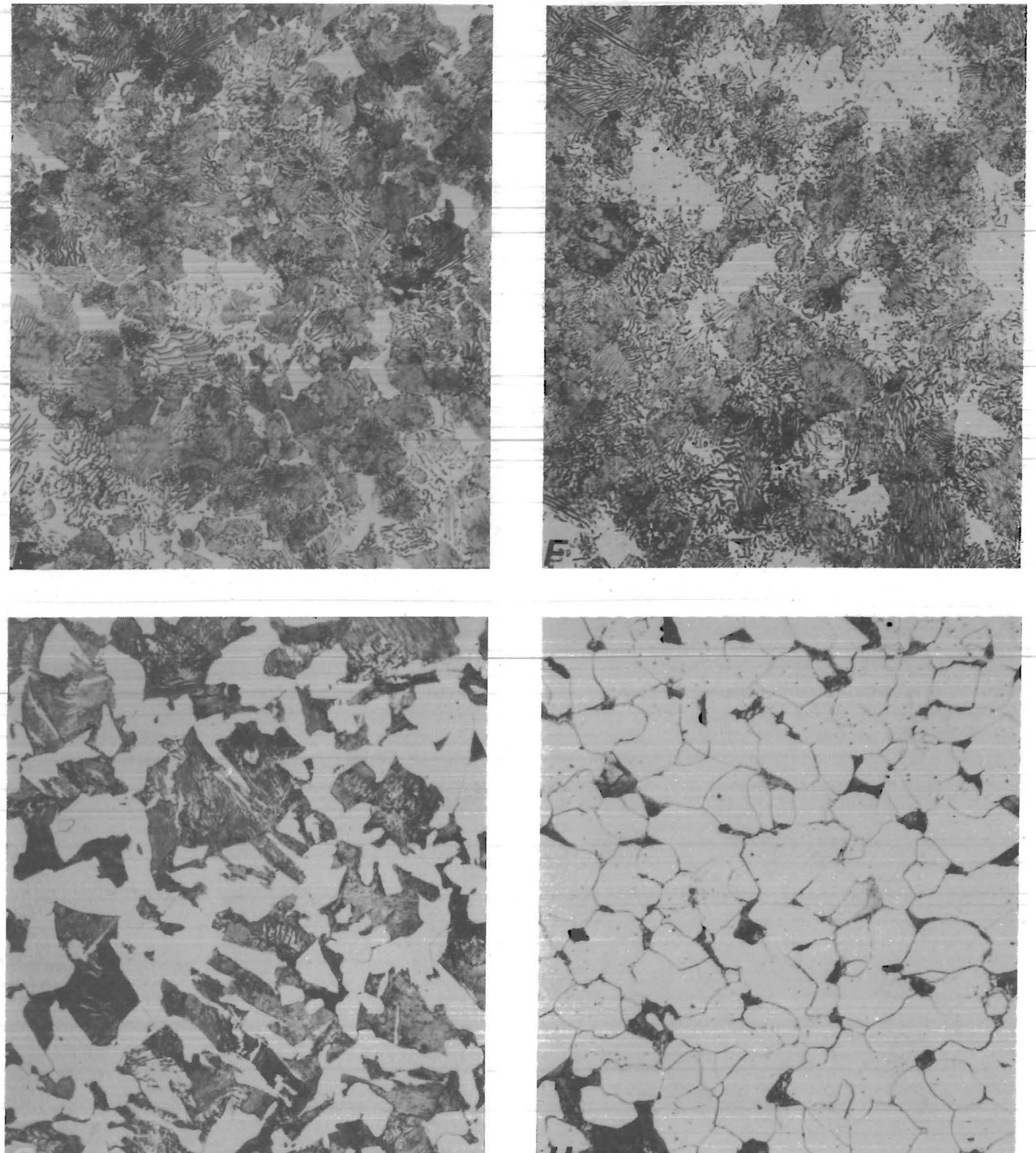


**FIGURE 1.—Microstructures of carbon and alloy steels (X 500)—Continued. AISI designations: *E*, 4140; *F*, 4340; *G*, 1035; *H*, 1020.**

TABLE 1. - Specific damping capacities and microstructures of carbon and alloy steels

| Steel, AISI[1] | Specific damping capacity, pct | | | | | Microstructure |
|---|---|---|---|---|---|---|
| | 2,500 psi | 5,000 psi | 10,000 psi | 15,000 psi | 20,000 psi | |
| 1045.. | 0.2 | 0.2 | 0.3 | 0.4 | 0.5 | Rounded colonies of fine lamellar pearlite in ferrite matrix. |
| 1144.. | .3 | .4 | .6 | .8 | .9 | Do. |
| 1095.. | .3 | .5 | .7 | .9 | 1.5 | Mostly unresolved pearlite with some lamellar spacing. |
| 1117.. | .6 | .9 | 1.1 | 1.0 | 1.0 | Rounded colonies of unresolved pearlite in predominant ferrite. |
| 4140.. | .3 | .8 | 1.6 | 3.9 | 8.4 | Fine-to-coarse lamellar pearlite in ferrite matrix. |
| 4340.. | .5 | 1.1 | 1.9 | 2.9 | 5.3 | Do. |
| 1035.. | .7 | 1.1 | 1.9 | 2.9 | 8.1 | Sharp-faceted colonies of fine lamellar pearlite in ferrite matrix. |
| 1020.. | 1.5 | 2.0 | 2.1 | 2.1 | 2.9 | Limited pearlite in large, sharp-faceted grains of ferrite. |

[1]Microstructures are shown in figure 1.

matrix (1117). Damping for the AISI 4140, 4340, 1035, and 1020 steels was higher. They were characterized by lamellar pearlite colonies with fine-to-coarse spacing in ferrite (4140 and 4340), coarse grained structure of sharp-faceted pearlite in a matrix of ferrite (1035), and reduced quantities of sharp-faceted pearlite in ferrite matrix (1020).

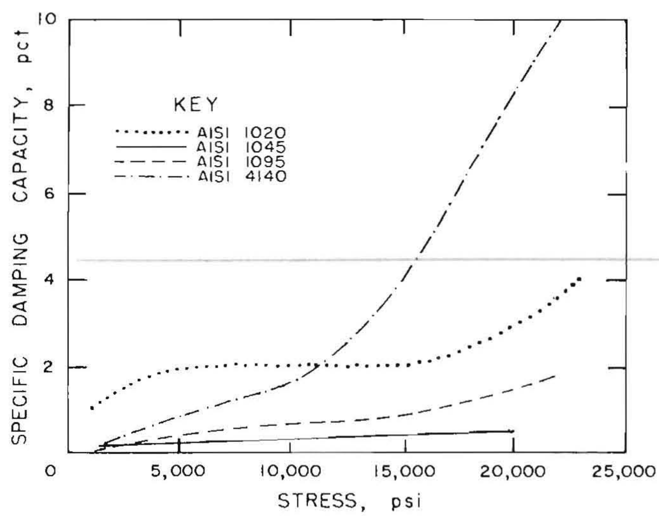


FIGURE 2.—Specific damping capacity of carbon and alloy steels as a function of stress.

The damping capacities of three of five specimens were improved by carburizing and spheroidizing heat treatment, which altered the carbide morphology. Table 2 summarizes the SDC's of the five specimens, and figure 3 shows their corresponding carbide morphologies. It is evident from the photomicrographs in figure 3 that, in all cases, the lamellar pearlite was converted to partly spheroidized pearlite and spheroidal cementite.

SDC's for all carbon steels (1045, 1095, and 1144) improved, especially at stress levels above 10,000 psi. All of these steels had rather low initial SDC's, and spheroidizing improved the SDC by a factor of 2 at the 5,000-psi stress level and by as much as tenfold at the 20,000-psi stress level. The SDC of the 4140 alloy steel did not change, but this material exhibited high damping prior to the heat treatment. The SDC of the 4340 alloy steel decreased somewhat in the 10,000- to 20,000-psi stress range, although this alloy also showed good

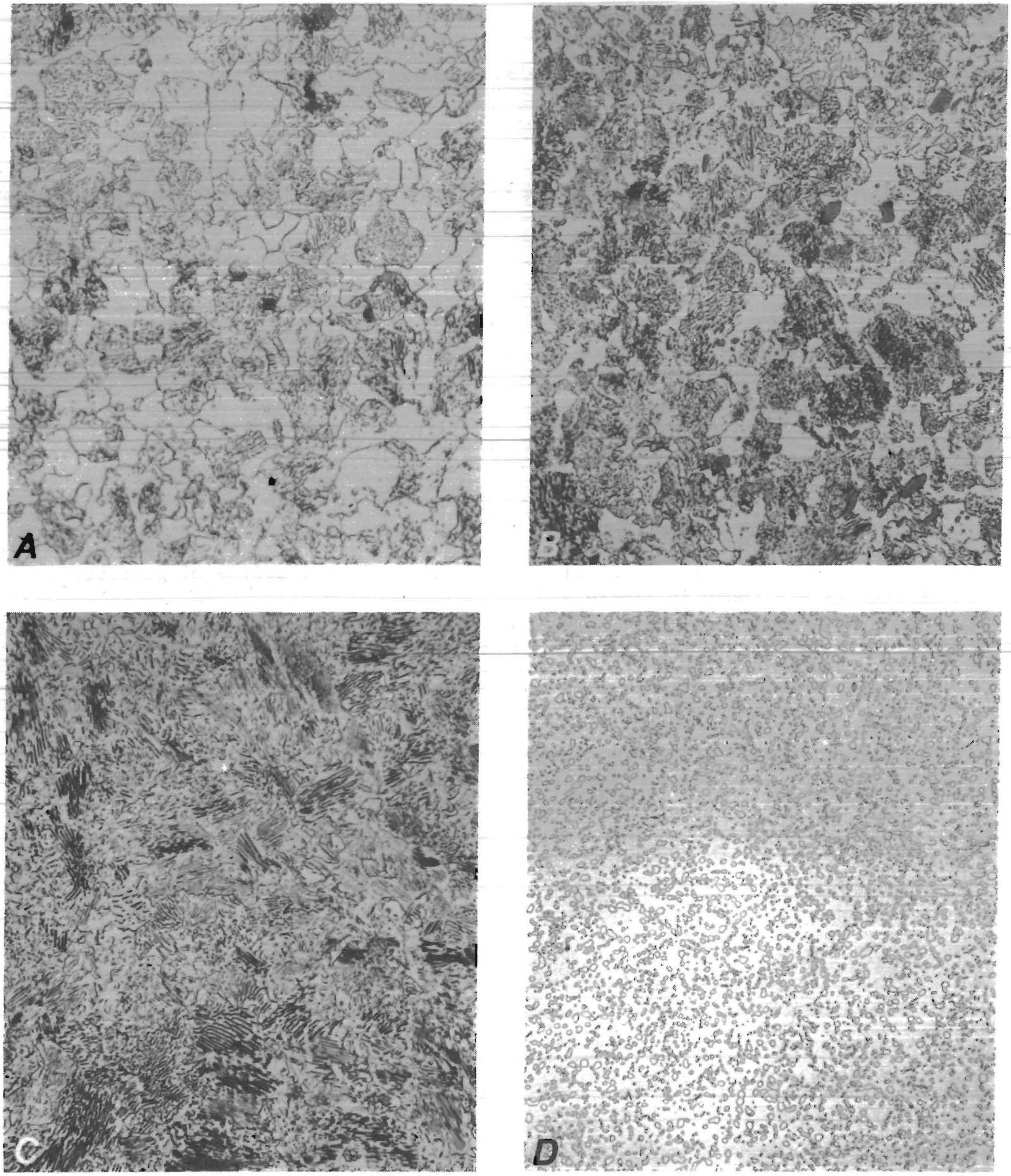


FIGURE 3.—Microstructures of spheroidized heat-treated carbon and alloy steels (X 500). AISI designations: *A*, 1045; *B*, 1144; *C*, 1095; *D*, 1095 (fully spheroidized).

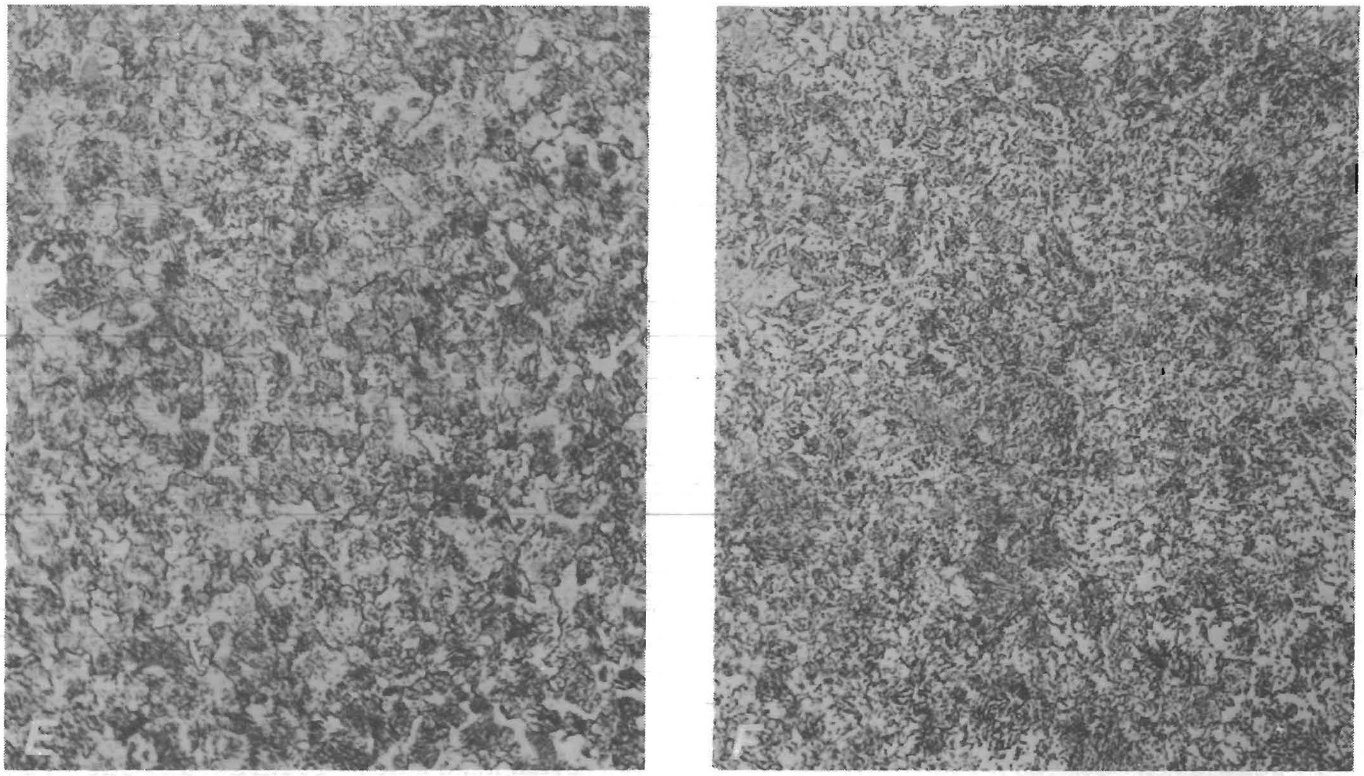

FIGURE 3.—Microstructures of spheroidized heat-treated carbon and alloy steels (X 500)—Continued. AISI designations: *E*, 4140; *F*, 4340.

TABLE 2. - Specific damping capacities of spheroidized heat-treated carbon and alloy steels

| Steel, AISI[1] | Specific damping capacity, pct | | | | | Spheroidized heat treatment |
|---|---|---|---|---|---|---|
| | 2,500 psi | 5,000 psi | 10,000 psi | 15,000 psi | 20,000 psi | |
| 1045... | 0.9 | 2.0 | 3.9 | 13.0 | ND | 6-h hold at 750° C, 36-h hold at 660° C. |
| 1144... | 2.0 | 4.4 | 8.6 | 28.8 | 44.2 | Do. |
| 1095... | .7 | 1.2 | 2.1 | 4.5 | 8.3 | 6-h hold at 715° C, 36-h hold at 680° C. |
| 1095[2].. | 1.2 | 2.1 | 4.0 | 5.4 | 6.4 | Unknown. |
| 4140... | .3 | .8 | 1.6 | 3.9 | 8.4 | 6-h hold at 750° C, 36-h hold at 660° C. |
| 4340... | .2 | .5 | 1.6 | 2.2 | 3.1 | Do. |

ND Not determined.
[1]Microstructures are shown in figure 3.
[2]Fully spheroidized.

damping before heat treatment. For comparison, the SDC of a fully spheroidized 1095 steel is included in table 2, and a photomicrograph of this steel is presented in figure 3.

The results of the SDC measurements on selected carbon and alloy steels indicate that damping is primarily dependent on the shape of the intergranular boundaries and the distribution of ferrite in the matrix. For steels characterized by a defined intergranular boundary between the pearlite colonies and ferrite matrix or grains, damping increases as intergranular boundary surfaces become rougher, thus producing higher stress concentrations. When the steels are heat treated, the pearlite colonies tend to lose their identity as the lamellar carbides begin to spheroidize and the ferrite agglomerates into a more continuous form. It is surmised that as the grain boundaries disappear during spheroidization, they lose their influence on damping, and the stress concentrations associated with the phase boundaries become predominant. For a given carbon content, more phase-boundary surface area is present for partially spheroidized carbides than for fully spheroidized carbides. Partially spheroidized particles are more sharply faceted and would tend to exhibit higher damping. As spheroidization increases, the total cementite surface area becomes smaller and smoother, whereas the ferrite becomes more continuous. The decrease in surface area and increased smoothness would tend to decrease damping; whereas, increased ferrite would tend to increase damping. This was observed in the AISI 1095 steels, where the partially spheroidized steel had higher damping at the 20,000-psi stress level than the fully spheroidized steel. Manipulating these parameters in steels can enhance, or also reduce, the inherent damping associated with them.

## CAST IRONS

The damping capacities of selected ductile, compacted graphite, and gray cast iron specimens were measured. Table 3 presents the SDC measurements for eight cast irons, and table 4 presents their compositions and mechanical properties. Figure 4 shows their etched microstructures. In the photomicrographs (~~fig.~~ 4), ferrite appears light; pearlite, dark gray; graphite, gray-to-black; and primary carbide particles, light. The eight cast irons were selected to demonstrate change in SDC with graphite morphology and are representative of all the cast irons tested. SDC-versus-stress curves are presented in figure 5 for two

TABLE 3. - Specific damping capacities and graphite morphologies of selected cast irons

| Specimen[1] | Graphite morphology[2] | Specific damping capacity, pct | | | | |
|---|---|---|---|---|---|---|
| | | 2,500 psi | 5,000 psi | 10,000 psi | 15,000 psi | 20,000 psi |
| A............. | N | 0.7 | 1.0 | 1.6 | 2.0 | 2.5 |
| B............. | N | 1.1 | 1.5 | 2.1 | 2.7 | 3.3 |
| C............. | N | 2.3 | 3.0 | 3.1 | 3.1 | 3.2 |
| D............. | N, C | 1.4 | 2.0 | 2.7 | 4.3 | ND |
| E............. | C, N | 1.9 | 2.9 | 4.3 | 5.8 | ND |
| F............. | C, N | 2.1 | 3.3 | 5.2 | 7.0 | ND |
| G............. | F | 4.1 | 5.7 | 9.2 | 12.5 | ND |
| H............. | F | 13.0 | 15.9 | 22.0 | ND | ND |

ND Not determined.
[1]Microstructures are shown in figure 4.
[2]C is compacted, N is nodular, and F is flake. Predominant form listed first.

TABLE 4. - Composition and mechanical properties of selected cast irons

| Specimen[1] | Analysis, wt pct | | | | | | | | Strength, psi | | Elongation, pct |
|---|---|---|---|---|---|---|---|---|---|---|---|
| | C | Si | Mn | S | Mg | Ce | Zr | Ti | Tensile | Yield | |
| A........... | 3.55 | 2.22 | 0.55 | 0.016 | 0.035 | ND | ND | ND | 79,600 | 48,200 | 10.5 |
| B........... | 3.22 | 2.46 | .29 | .005 | .016 | ND | ND | ND | 65,200 | 41,900 | 18 |
| C........... | 3.22 | 2.46 | .29 | .005 | .016 | ND | ND | ND | ND | ND | ND |
| D........... | 3.84 | 2.37 | .30 | .002 | ND | 0.015 | 0.060 | ND | 61,900 | 44,100 | 7.5 |
| E........... | 3.84 | 2.76 | .31 | .002 | ND | .012 | .070 | ND | 55,300 | 41,900 | 5.5 |
| F........... | 3.82 | 2.79 | .29 | .004 | ND | .014 | ND | 0.240 | 51,600 | 40,700 | 3 |
| G........... | 3.61 | 2.64 | .24 | .005 | .007 | ND | ND | .120 | 26,600 | 23,800 | 1 |
| H........... | 3.74 | 2.68 | .29 | .007 | ND | .008 | ND | .070 | 25,300 | 21,900 | 1.5 |

ND Not determined. [1]Microstructures are shown in figure 4.

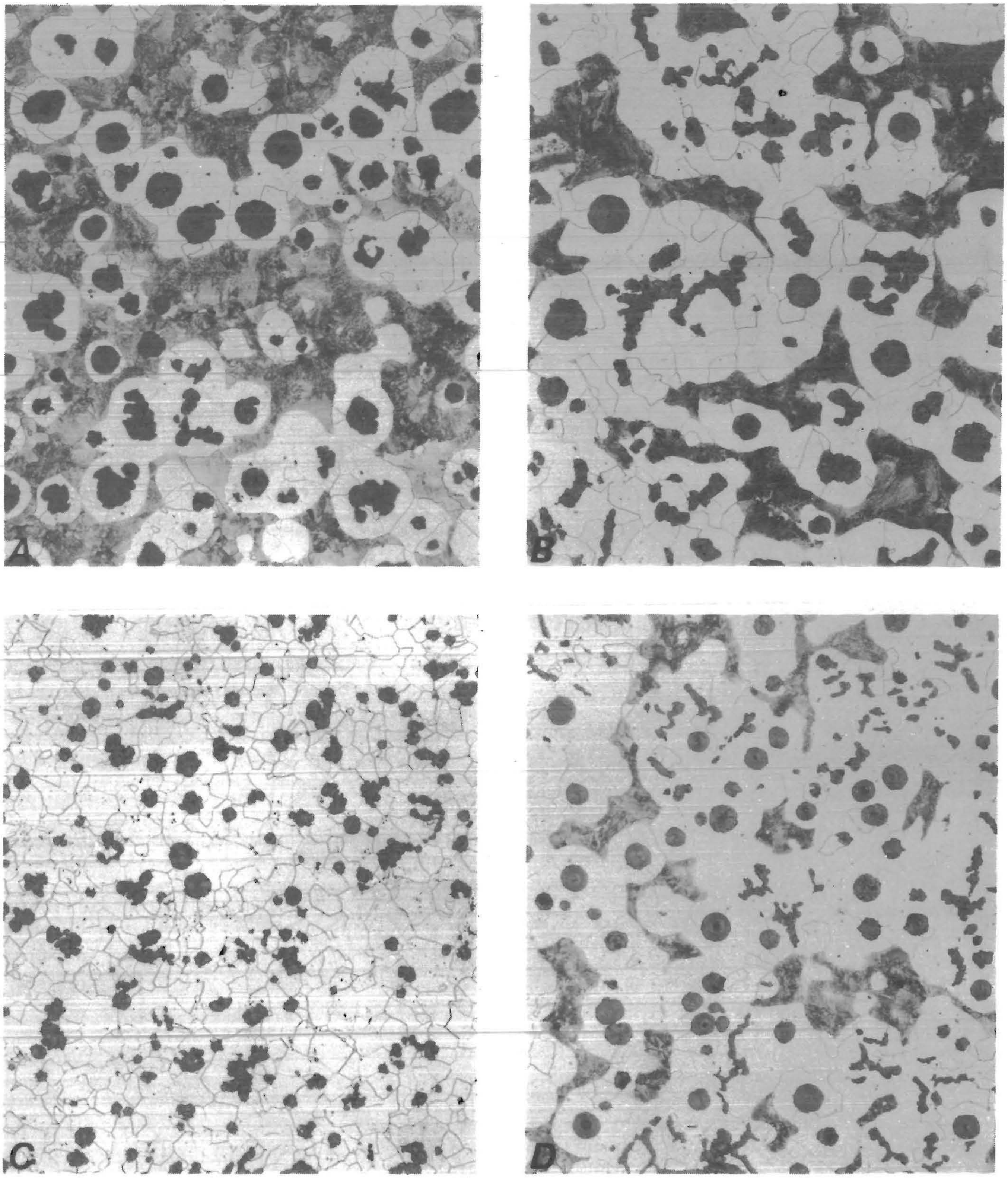


FIGURE 4.—Microstructures of cast irons (X 100). Specimens *A* through *D* as listed in tables 3 and 4. See text for description of microstructures.

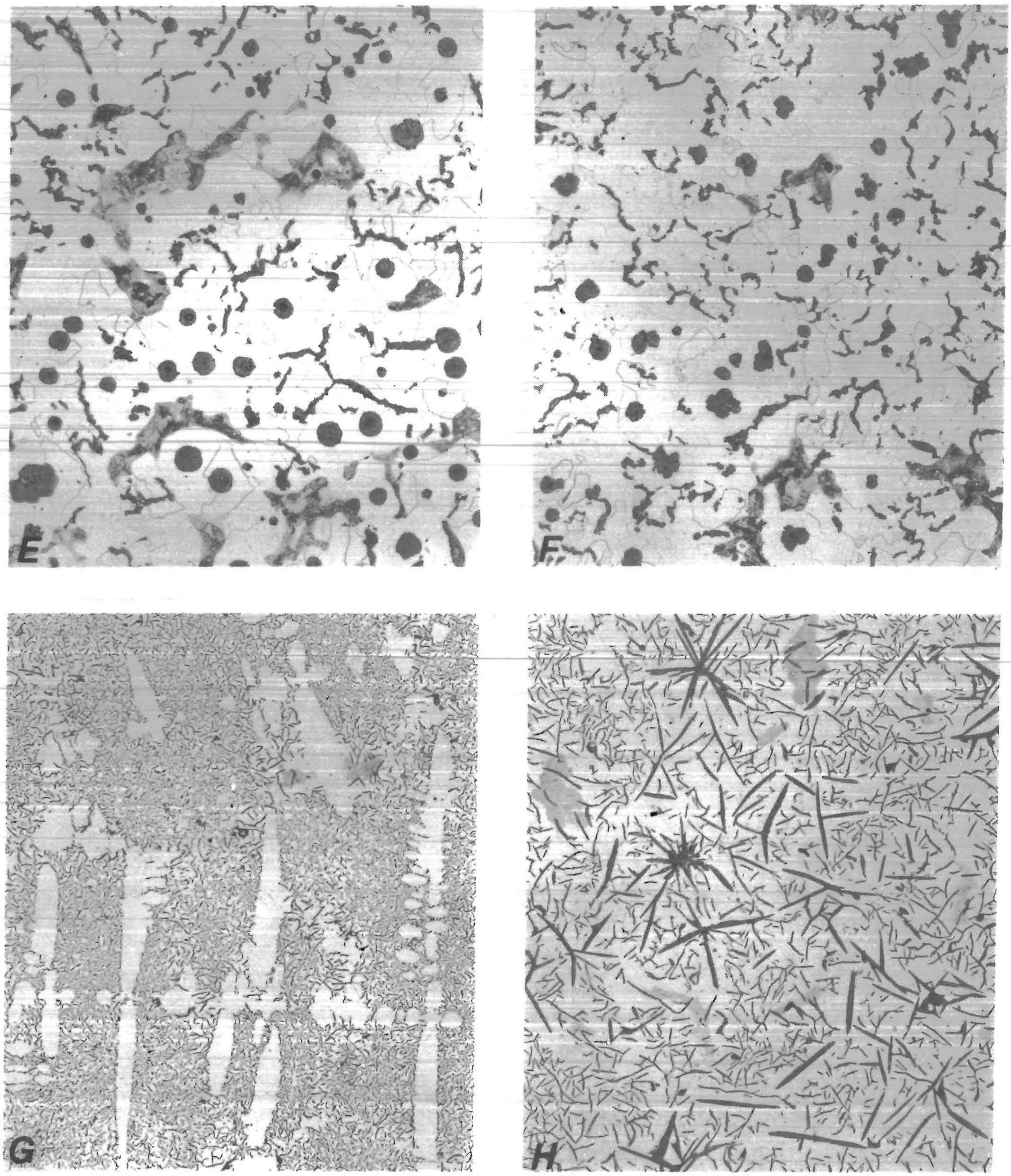


FIGURE 4.—Microstructures of cast irons (X 100)—Continued. Specimens *E* through *H* as listed in tables 3 and 4. See text for description of microstructures.

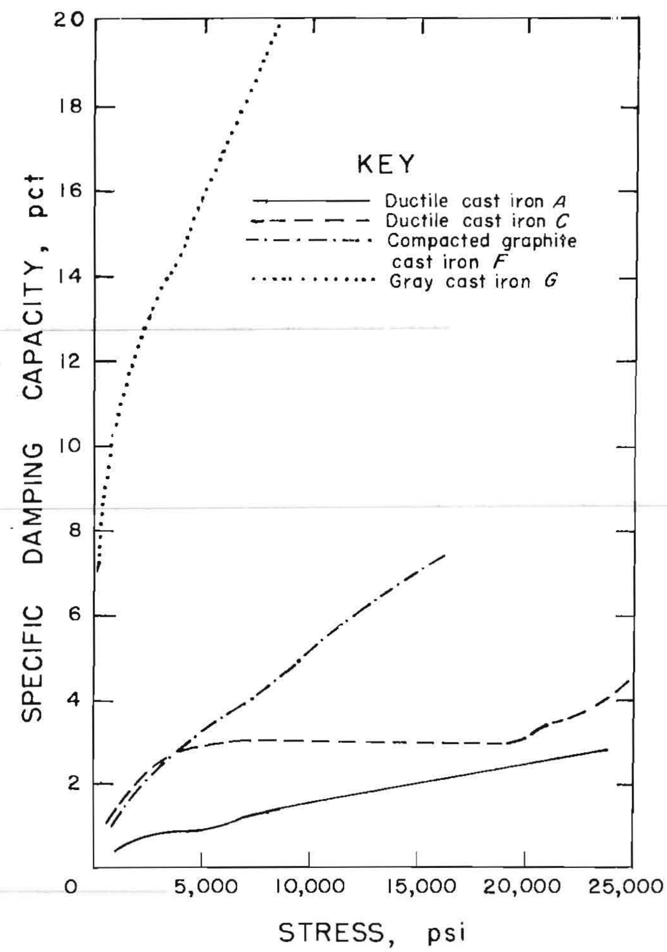


**FIGURE 5.—Specific damping capacity of cast irons as a function of stress. Letters in key indicate specimens listed in tables 3 and 4 and shown in figure 4.**

ductile, one compacted graphite, and one gray cast iron (four of the eight selected cast irons). Specimens *A*, *B*, and *C* (fig. 4) were ductile irons with graphite nodules in a pearlite-plus-ferrite matrix, graphite nodules in ferrite and some pearlite, and graphite nodules in a ferrite matrix, respectively. Specimen *C* was produced from the same casting as specimen *A* by ferritize-annealing. The increase in SDC as a function of increased ferrite matrix is readily apparent from the data in table 3. Specimen *B*, which had more ferrite and less pearlite than specimen *A*, exhibited from 1.6 to 1.3 times the SDC of specimen *A*. The ferritize-annealed specimen *C* with the ferrite matrix exhibited from 3.3 to 1.3 times the SDC of specimen *A*. In the case of specimen *C*, the most pronounced increase in SDC was at the lower stress levels, which is most desirable from an engineering standpoint.

Ferritize-annealing decomposes hard-matrix $Fe_3C$ in the pearlite to softer ferrite plus graphite. The graphite deposits on the existing graphite nodules. Although precise mechanisms are not clear, a softer condition of the matrix and the additional graphite, which increased the area associated with grain boundaries, would be expected to increase stress concentrations. This would be more effective than the straight cast structure in dissipating rather than storing strain energy in the matrix and thus improving the damping capacity.

Specimens *D*, *E*, and *F* (fig. 4) were castings that contained compacted graphite and some nodular graphite, with the proportion of compacted graphite to nodular graphite increasing from specimen *D* to *F*. All specimens also contained isolated patches of pearlite in the ferrite matrix. SDC's for these cast irons (*D*, *E*, and *F*) at all stress levels (table 3) increased in the same sequence as the increase in compacted graphite. SDC at the 2,500-psi stress level ranged from 1.4 to 2.1 pct, which was two to three times greater than the SDC for ductile iron specimen *A*. Similar improvement in SDC was evident at all the stress levels listed in table 3, and SDC at the 15,000-psi stress level ranged from 4.3 to 7.0 pct for these three specimens.

The highest SDC's were observed for specimens *G* and *H*, which consisted of gray cast iron with a flake graphite microstructure. Specimen *G* was a gray cast iron with type D (interdendritic segregation and random orientation) graphite distribution, and it exhibited SDC's approximately six times higher than those of ductile cast iron specimen *A*. Specimen *H* had a type C (superimposed flake size and random orientation) graphite distribution, and its SDC values ranged from 14 to 18 times higher than those of ductile cast iron specimen *A*.

Compacted graphite has a "wormy" appearance intermediate between the appearances of nodules and flakes. It is a distinct type in that it is continuous in the bulk matrix, as are the flakes of gray cast iron; but, compared with the sharp edges of flakes, the rounded edges are less effective for stress concentration and resultant vibration energy dissipation. For a given matrix, these rounded edges account, to a large extent for the SDC of compacted graphite cast iron falling between those of ductile and gray cast iron.

Comparison of the cast iron damping capacities in table 3 with the mechanical properties in table 4 indicates an inverse relationship between SDC and elongation and tensile and yield strength. SDC increases as percent elongation and tensile and yield strength decrease. This is not unexpected, because the trend follows the sequence of graphite morphology from nodular to compacted to flake or their various combinations. Thus, in the absence of SDC data for cast irons, elongation and tensile and yield strength information can be used to arrive at an estimate of their damping capabilities.

## CONCLUSIONS

The steels and cast irons investigated here represent only a small fraction of the carbide and graphite morphologies possible for these materials. The intent of the study was to provide baseline damping capacity data for some common structural and engineering materials, and to determine relationships between damping capacity and material microstructure. The results indicate that damping in both the steels and cast irons examined is strongly dependent on the level of stress associated with the intergranular boundaries and the presence of ferrite in the matrix. Damping improves with rougher intergranular contact, increased ferrite, or their various combinations. Heat treatments that accentuate these conditions in the matrix increase damping. Compared to carbon and alloy steels, cast irons even with the lowest SDC's exhibit better damping in most cases. The SDC of some alloy steels can be increased to the level of cast iron SDC's by heat treating.

## REFERENCES

1. Jensen, J. W., and D. F. Walsh. Manganese-Copper Damping Alloys. BuMines B 624, 1965, 55 pp.

2. Holman, J. L., R. L. Crosby, and L. A. Neumeier. Properties of Manganese-Copper Alloys Prepared From Metal Powders. BuMines RI 8383, 1979, 32 pp.

3. Birchon, D. Hidamets--Metals to Reduce Noise and Vibration. Min. Eng. (London), v. 222, Aug. 1966, pp. 207-209.

4. Fister, J. C., and J. F. Breedis. Improved High Damping Copper-Base Alloys. Int. Copper Res. Assoc., New York, NY. INCRA Final Rep. 221, Jan. 1976, 32 pp.

5. Nachman, J. F., and A. N. Hammer. Characteristics of Commercial Incramute I. Int. Copper Res. Assoc., New York, NY. INCRA Rep. RDR 1713, Nov. 1971, 12 pp.

6. Nachman, J. F., C. Napier, and A. N. Hammer. Development of Cu-Mn Base Alloys With High Damping Properties. Int. Copper Res. Assoc., New York, NY. INCRA Final Rep. 152-152A, March 1971, 23 pp.

7. Toshiba Research and Development Center. Silentalloy SIA Technical Data. Tokyo Shibaura Electric Co., Ltd., Kamukai, Kawasaki, Japan, 13 pp.

8. Clarke, H. Effect of Pore Geometry on the Damping Characteristics of Sintered Irons. Paper in Modern Developments in Powder Metallurgy, v. 11, P/M Special Materials and Applications, ed. by H. H. Hausher and P. V. Taubenblat (Proc. 1976 Int. Powder Met. Conf., Chicago, IL, June 27-July 2, 1976). Metal Powder Ind. Fed., Princeton, NJ, pp. 385-395.

9. Cowen, P. S. Part 1: Heat Treatment of Ductile Iron Castings. Foundry, v. 99, No. 9, 1971, pp. 60-63.

10. Cowen, P. S. Part 2: Heat Treatment of Ductile Iron Castings. Foundry, v. 99, No. 10, 1971, pp. 78-81.

11. American Society for Testing and Materials. Standard Method and Definitions for Mechanical Testing of Steel Products. ANSI/ASTM A370-77 in 1981 Annual Book of ASTM Standards: Part 2, Ferrous Castings; Ferroalloys. Philadelphia, PA, 1981, pp. 187-242.

12. Schwaneke, A. E., and R. W. Nash. An Improved Torsion Pendulum for Measuring Internal Damping. Rev. Sci. Instrum., v. 40, 1969, pp. 1450-1453.

13. Nash, R. W., and A. E. Schwaneke. A Digital Instrumentation Package for an Improved Torsion Pendulum. BuMines RI 8774, 1983, 9 pp.

U.S. GOVERNMENT PRINTING OFFICE: 1987 - 605-017/60011

INT.-BU.OF MINES,PGH.,PA. 28400